Supplementary Information for the manuscript titled "Effect of surfactant on the settling of a drop towards a wall"

Sayali N. Jadhav[1] and Uddipta Ghosh[1]

[1]*Department of Mechanical Engineering, Indian Institute of Technology Gandhinagar, Palaj - 382355, Gujarat, India*

This supplementary information is divided into four distinct sections. In §S1, we assess the "Quasi-steady state" assumption undertaken in our analysis. This section also includes a discussion on the added mass effect in relation to eqn. (4.13) in the manuscript. In §S2, the solution convergence is tested. This justifies the truncation of the infinite series that appear as the solutions to the stream function and other related quantities, as outlined in §4.1 of the manuscript. §S3 is dedicated to the influence of the parameter k on the settling velocity of the drop. Finally, in §S4, flow visualization in and around the drop through streamline plots at various stages of settling are presented. §S4 also contains a brief discussion (in continuation to figure 5 in the manuscript) on how the surfactant gets redistributed around the drop interface, when it is very close to the wall.

S1 Assessment of the Quasi-Steady flow assumption

S1.1 The time scales of the problem

We have outlined in §2 of the manuscript that the drop motion has been assumed to be quasi-steady. This assumption plays a key role in determining the net hydrodynamic drag acting on the drop. At its core, the quasi-steady approximation says that the viscous stresses can quickly readjust in response to any other changes in the flow, which is why the temporal term in the LHS of the Navier-Stokes equation can be dropped. This can be better understood from the non-dimensional governing equation for fluid motion, expressed as:

$$Re\left(\frac{1}{S}\frac{\partial \mathbf{u}}{\partial t} + \mathbf{u}\cdot\boldsymbol{\nabla}\mathbf{u}\right) = \nabla^2\mathbf{u} - \boldsymbol{\nabla}p \tag{S1}$$

where Re is the Reynolds number ($Re = U_c a/\nu$, see §3 in the manuscript) and $S = t_0/t_a$ (also called the Strouhal number) is the ratio of the char. time scale of the flow to advection time scale (a/U_c). In the present scenario, $t_0 = t_a$ is the most appropriate choice and hence $S = 1$. It is evident that the inertial terms in the eqn. (S1) may be neglected when $Re \ll 1$, which indicates that the flow is dominated by viscous stresses [1]. This assumption remains a cornerstone in many seminal studies on droplet and particle dynamics [2, 3] in viscous fluids.

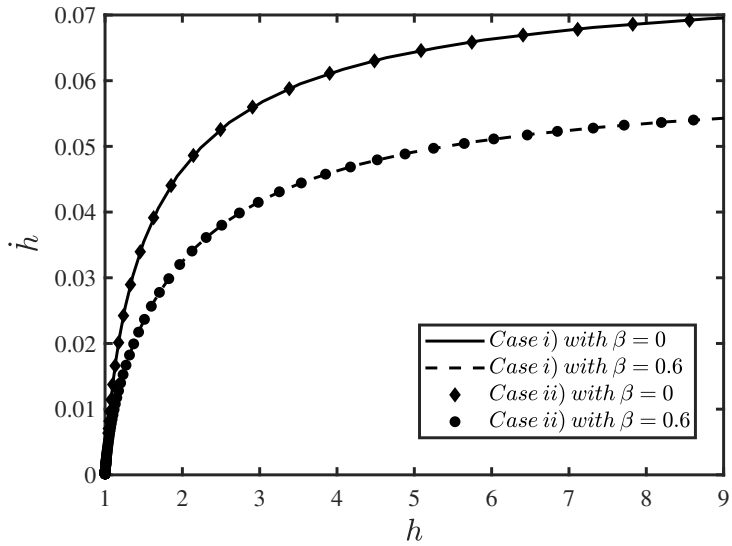

Figure S1: Phase plot of settling ($\dot{h}$ vs h) with two different initial conditions for velocity: i) $h = 10$, $\dot{h} = 0$ (represented by solid curves), ii) $h = 10$, $\dot{h} = U_o$ (represented by dashed red curves), for $\beta = 0, 0.6$, $\lambda = 0.1$ and $k = 3$.

S1.2 Added mass effect and the effect of initial acceleration

In case of large accelerations, the temporal derivative in the Navier-Stokes equation (the $\partial u/\partial t$ term) may be retained, despite the Reynolds number being small. This leads to a modification in the force acting on the particle. For a solid spherical particle of radius a, moving in a straight line with arbitrary velocity $u(t)$ in a fluid with density ρ and kinematic viscosity ν, the hydrodynamics drag force has the form [4, 5]:

$$F = 2\pi\rho a^3 \left(\frac{3\nu u}{a^2} + \frac{1}{3}\frac{du}{dt} + \frac{3}{a}\sqrt{\frac{\nu}{\pi}} \int_{-\infty}^{t} \frac{du}{d\tau} \frac{d\tau}{\sqrt{t-\tau}} \right) \tag{S2}$$

The second term inside the bracket is usually termed as the "Added mass effect", while the first term is the usual Stoke's drag. Clearly, the second and the third terms become important, when the velocity of the particle changes rapidly, in the viscous flow limit. Such scenarios usually occur for gas bubbles moving through liquids [6], because of its negligible mass and thus taking into account added mass makes sense there. On the contrary, in our study, quasi-steady flow is considered and as a result the temporal derivative is neglected here (see eqn. (3.6) in the manuscript and eqn. (S1) above) on account of the fact that the char. time scale here is precisely equal to the advection time scale i.e. $t_c = t_a = a/U_c$, making $S = 1$. As a result, when $Re \ll 1$, one can drop the entire LHS in eqn. (S1). Therefore, consideration of added mass effect, like that in (S2) would be incompatible with the quasi-steady assumption.

Further, large initial acceleration will not play an important role in the present scenario since the densities of droplet and surrounding fluids are close ($\rho_2/\rho_1 = 1.1$). To verify this, we have now analyzed whether the initial acceleration has any significant effect on droplet motion. This may be done by solving eqn. (4.13) in the manuscript using two different sets of initial conditions. The first set of solutions has the initial conditions, $h = 10$ and $\dot{h} = 0$ at $t = 0$, while the second set satisfies, $h = 10$, $\dot{h} = U_0$, at $t = 0$, where U_0 is the steady state velocity of the drop away from the wall. Therefore, in the first case, the drop will accelerate initially to reach the steady state velocity away from the wall, following which it will slow down. On the other hand, in the second case, the drop will not undergo any initial acceleration, since it was already settling at the steady state velocity. By comparing these two solutions, we can check whether

the initial acceleration plays an important role in governing the droplet's motion. Figure S1 shows this comparison as a phase plot ($\dot{h}$ vs h has been plotted here) for two different values of β (0 and 0.6), while values of other relevant parameters have been mentioned in the caption. It can be observed that both the initial conditions imposed on $\dot{h}$ result in the same phase plots, therefore confirming our earlier assertion that the initial acceleration is not a key factor here and hence the added mass effect can be safely neglected. At the same time, figure S1 also confirms the validity of the quasi-steady state assumption, central to the analytical solutions written in the manuscript.

S2 Solution Convergence

The solution for the stream functions, surfactant concentration gradient, drop velocity and deformation are represented in terms of infinite series of Legendre or Gegenbauer polynomials in our analysis (see §4 of the manuscript). Thus determining the convergence criteria for these infinite series becomes an important step in the solution procedure. Since the solution for the droplet settling velocity plays a key role in all other aspects of the problem, it is justified to focus on how the values (numerical) of U converge at various distances from the wall. We shall particularly emphasize on the scenario when the drop is very close to the wall (i.e. $h \to 1$ or, $h - 1 \ll 1$), because series convergence is likely to be poor there. As such, the expression for

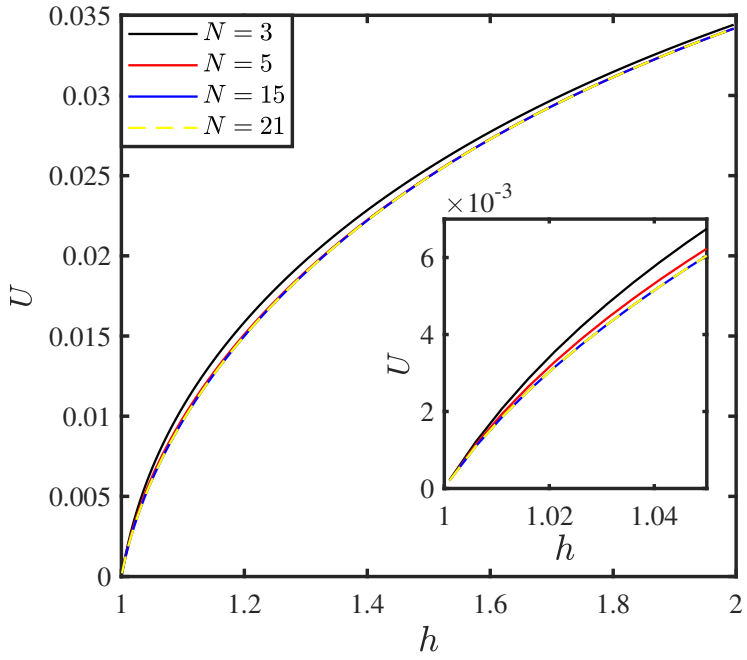

Figure S2: U (droplet settling velocity) vs h (normalized distance of the drop centre from the wall) for different truncation limits (N). Other relevant parameters are: $\beta = 0.5$, $\lambda = 0.1$ and $k = 3$. The inset shows magnified plot very close to the wall (i.e. $h \to 1$).

the instantaneous settling velocity of the drop is given as (see eqn. (4.12) in the manuscript):

$$U = \frac{1}{\pi\, 2\sqrt{2}c \sum_{n=0}^{\infty} (A_n + B_n + C_n + D_n)} \tag{S3}$$

Where, c is a constant of bipolar coordinate system (defined in §4 of the manuscript) and A_n, B_n, C_n, D_n are the coefficients in the infinite series for stream functions, found by solving

the coupled system of infinite linear equations (see §A.1 in the Appendix A of the manuscript). In practice, the summation in eqn. (S3) has to be truncated at an upper limit, say, N. After truncation, eqn. (S3) may be written as:

$$U = \frac{1}{2\sqrt{2}\pi c \sum_{n=0}^{N} (A_n + B_n + C_n + D_n)} \tag{S4}$$

Convergence of the series may be checked by choosing successively larger N-values and observe the resulting change in U. Figure S2 plots the droplet settling velocity (U) vs distance of the droplet center from the wall (h) for different choices of truncation limits (N) of the series given in eqn. (S4). One can clearly observe that the error in the solution for U consistently gets smaller as N is increased; this remains true for all values of h, i.e., the drop centre height. In other words, the changes in the numerical values of U become imperceptible, when $N \geq 15$. The inset depicts the convergence very close to the wall and again the trends described above are repeated there. In view of the above, in the manuscript, we have decided to truncate the series in eqn. (S3) after $N = 15$ terms.

S3 Effect of the parameter k on surfactant concentration

The primary focus of our analysis is to assess the influence of surfactant on the flow dynamics as well as motion and deformation of the drop. The extent of influence of the surfactant depends on the following parameters: (a) the surface tension coefficient β, (b) surfactant Péclet number, Pe, which in turn depends on the factor k (defined in §3 of the manuscript). The effect of β is analyzed in the manuscript (see §5 in the manuscript).

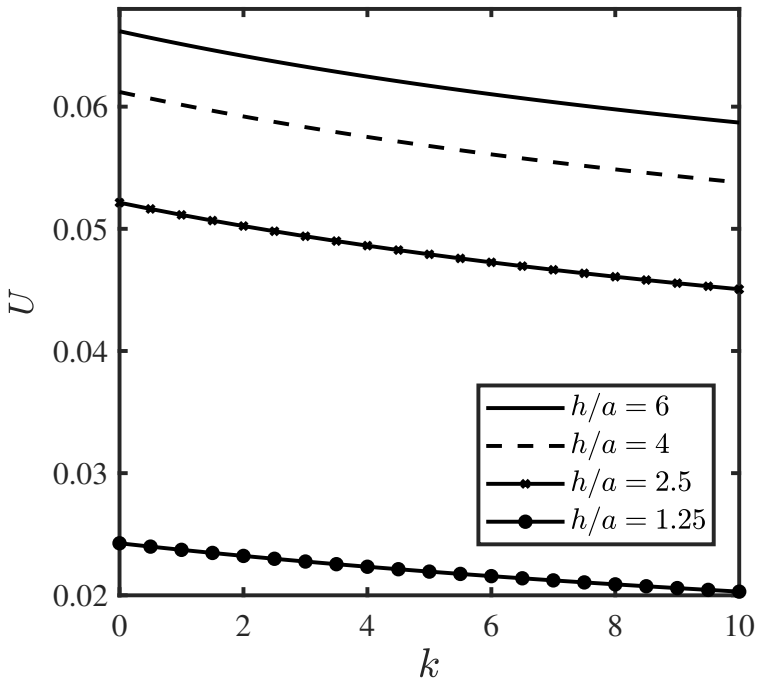

Figure S3: Plot of droplet settling velocity (U, found from eqn. (S3)) as a function of k for four different locations of the drop center, given by: $h = 6, 4, 2.5, 1.25$. Other relevant parameters are given by $\lambda = 0.1$ and $\beta = 0.1$.

The effect of varying k can be observed from figure S3, where droplet settling velocity (U, from eqn. (S3)) is plotted as a function of k, at four different locations of the drop center,

given by: $h = 6, 4, 2.5, 1.25$. Other relevant parameters are mentioned in the caption. From the figure it is clear when k increases, the settling velocity decreases at all distances from the wall. Increasing k augments the Marangoni stress contribution through the factor ω ($= \beta k/(1-\beta)$, see eqn. (4.5c) in the manuscript), which enhances the drag force on the drop, resulting in a decrease in the settling velocity. Note that these trends of U vs k are almost identical to the U vs β trends depicted in Fig. 3 in the manuscript. This is expected because, increasing β, keeping k constant, augments the effect of surfactants on surface tension, which ultimately results in increased drag. On the other hand, if one increases k by keeping β constant, the deviation in the surfactant concentration itself (Γ_1, see eqn. (3.11) in the manuscript) increases, which also enhances the variation in surface tension, thus leading to a very similar increase in the drag force.

S4 Physical perspectives on film drainage

S4.1 Surfactant distribution close to the wall

The effect of the bounding wall on the redistribution of surfactants has been discussed in relation to figure 5 in the manuscript. From that figure, it was observed that the surfactant concentration tends to become more uniform as the drop approaches the wall. At the same time, the deviation in Γ around its equilibrium value becomes asymmetric with relatively larger depletion near the southern pole. These trends are expected to continue as the drop settles towards the wall. During the film drainage ($h \to 1$), the interface velocity becomes very small owing to a rapid increase in the hydrodynamic drag. As a result, it is expected, that Γ will be very close to 1 almost everywhere on the interface, while the foresaid asymmetry will also

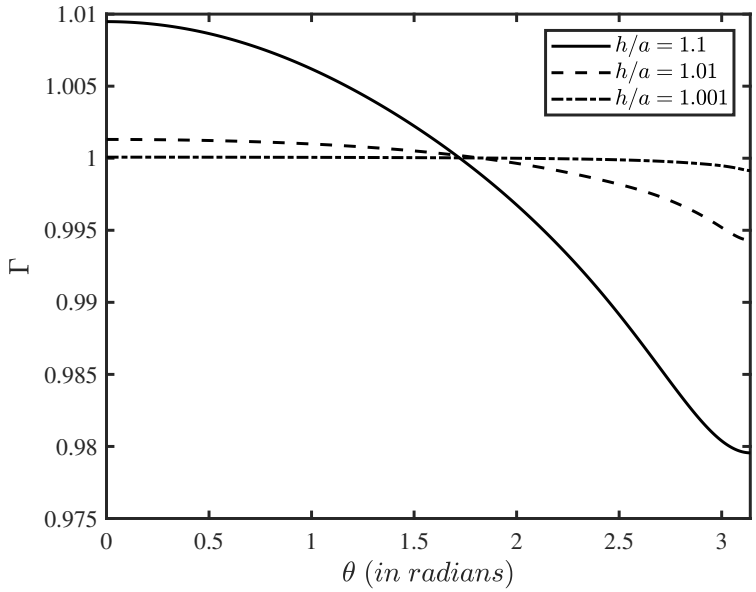

Figure S4: Plot of Γ vs θ, for three different locations of the drop, $h = 1.1,\ 1.01$ and 1.001. Other parameters are: $\beta = 0.1,\ Ca = 0.3,\ k = 3$ and $\lambda = 0.1$. Here, θ is the polar angle measured in a spherical coordinate system fixed at the drop center.

prevail. This is exactly what is observed in figure S4, where Γ as a function of polar angle θ has been plotted at three different locations of the drop, all very close to the wall. Values of other relevant parameters have been mentioned in the caption. Notice that at $h = 1.001$, the surfactant concentration is uniform throughout the drop interface, except near the south pole.

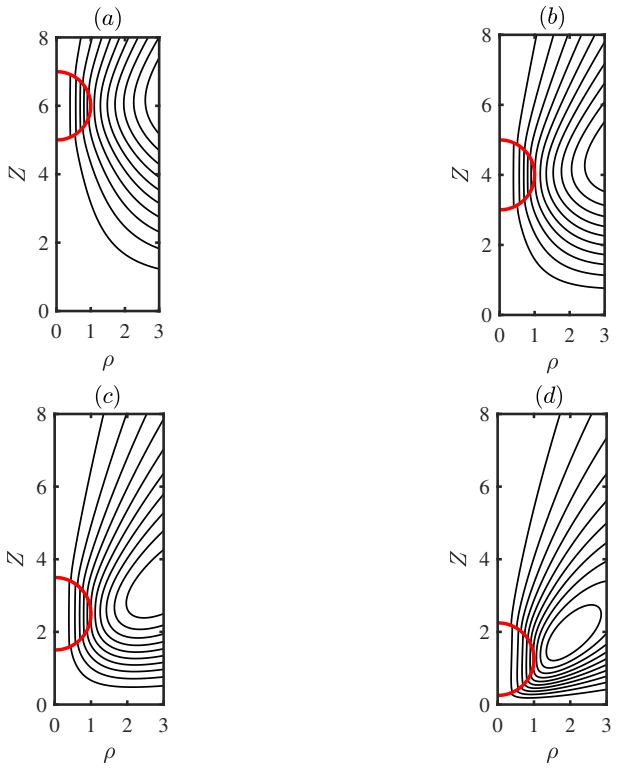

Figure S5: Streamline patterns emerging from the settling of the drop (with surfactant) in both the fluids have been shown here. We plot the streamlines at four different locations of the drop, given by (a)$h = 6$, (b) $h = 4$, (c) $h = 2.5$, (d) $h = 1.25$. The drop interface has been depicted with a thick red line. Values of other relevant parameters are: $\lambda = 1$, $k = 3$, $\beta = 0.9$.

S4.2 Flow pattern at various stages of settling

The flow dynamics in and around the drop as it settles towards the wall can be better visualized from streamline plots. To this end, in figure S5 (a) - (d), we showcase the streamlines in both the fluids for four different locations of the drop, given by $h = 6$ in (a), $h = 4$ in (b), $h = 2.5$ in (c) and $h = 1.25$ in (d), using eqns. (4.3) & (4.4) in the manuscript. Presence of surfactant is taken into account here with $\beta = 0.9$ and other relevant parameters have been mentioned in the caption. Note that in fig. S5, the drop surface has been shown by a red line. Observing all four subfigures, the effect of the bounding wall on the overall nature of the flow becomes clear. In subfigure (a), the influence of the wall on the flow around the drop is minimal as it is very similar to the flow in an unbounded medium. At this point, the wall, being impenetrable, mainly pushes the surrounding fluid (fluid-1) sideways as it rushes towards the wall because of the motion of the drop. As the drop nears the wall (see subfig. (b)), the same flow patterns persist, although now the streamlines become more curved, but still remain open, close to the drop. The aforementioned curvature of the streamlines becomes extreme at $h = 2.5$ (see subfig. (c)) as the outer fluid immediately turns sideways just below the drop. Within the region explored in the fig. S5(c), the streamlines still remain open. However, at $h = 1.25$ (see subfig. (d)), since the drop is very close to the wall, the extremely curved flow pathways give away to closed streamlines in the form of recirculation rolls. This, of course, is qualitatively different from the previous three subfigures where only open streamlines were visible. Essentially, the flow patterns shown in subfigure (d) are precursor to the final stages of settling, where film drainage takes place. It may be noted from this subfigure that the final traces of fluid-1 residing between the drop and the solid surface begins to squeeze out as the

drop nears the wall. The final stages of settling and the associated effect of the surfactant are best captured through the variations in film thickness (Δh), as it drains out from beneath the drop. A detailed account of this phenomena has been discussed in relation to figure 8 in the manuscript - see §5.3 therein. Further note that the streamline patterns inside the drop essentially remain unchanged at all four locations, as the flow therein is mainly dominated by the straight downward motion of the drop itself.

References

[1] John Happel and Howard Brenner. *Low Reynolds number hydrodynamics: with special applications to particulate media*, volume 1. Springer Science & Business Media, 2012.

[2] Howard Brenner. The slow motion of a sphere through a viscous fluid towards a plane surface. *Chemical engineering science*, 16(3-4):242–251, 1961.

[3] S Haber, G Hetsroni, and A Solan. On the low reynolds number motion of two droplets. *International Journal of Multiphase Flow*, 1(1):57–71, 1973.

[4] LD Landau and EM Lifshitz. *Fluid Mechanics: Course on Theoretical Physics, Vol. 6*. Pergamon Press, 1959.

[5] L Gary Leal. *Advanced transport phenomena: fluid mechanics and convective transport processes*, volume 7. Cambridge University Press, 2007.

[6] JB W Kok. Dynamics of a pair of gas bubbles moving through liquid. i: Theory. *European journal of mechanics. B, Fluids*, 12(4):515–540, 1993.